

# Resonant electron transfer and luminescent enhancement in a toluene suspension of Si nanocrystals

X. L. Wu,<sup>a)</sup> T. Qiu, D. S. Hu, G. S. Huang, and R. K. Yuan

*National Laboratory of Solid State Microstructures and Department of Physics, Nanjing University, Nanjing 210093, People's Republic of China*

G. G. Siu and Paul K. Chu

*Department of Physics and Materials Science, City University of Hong Kong, Kowloon, Hong Kong, China*

(Received 17 January 2005; accepted 20 June 2006; published online 3 August 2006)

Efficient resonant electron transfer from the surface bonding structure to the conduction band of quantum confined Si nanocrystals is observed by Si nanocrystals in a toluene suspension. Based on the electron transfer mechanism, the enhancement of photoluminescence originates from the band-to-band recombination in the *p*-type Si nanocrystals suspended in a toluene solution. The energy levels of the electrons in the Si nanocrystals chemisorbed with toluene molecules are calculated using the method of linear combination of atomic orbitals, and the characteristics of the obtained density of states is in good agreement with the observed photoluminescence properties. © 2006 American Institute of Physics. [DOI: [10.1063/1.2227384](https://doi.org/10.1063/1.2227384)]

## I. INTRODUCTION

In recent years, organic-inorganic hybrid optoelectronic nanomaterials have attracted considerable attention due to the remarkably fast charge transfer rates between organic molecules with relatively low ionization potential and inorganic semiconductors possessing high electron affinity.<sup>1-3</sup> Their light emitting properties have been investigated experimentally and improvement of luminescence efficiency and quenching of photoluminescence (PL) have been observed.<sup>4-9</sup> However, on account of the complex microscopic details in such an integrated structure, the light emitting mechanism is not well understood.

Toluene (C<sub>7</sub>H<sub>8</sub>) is one of the most important unsaturated aromatic hydrocarbons in organic chemistry and absorption of toluene on the Si (100) surface has been widely examined in recent years.<sup>10</sup> Using maximally localized Wannier functions, chemisorption of toluene on the Si (100) surface can be described as a proton abstraction reaction in which excess negative charge transfer occurs along a new C-Si bond to the Si atom.<sup>10</sup> According to the well established PL mechanism pertaining to inorganic nanomaterials,<sup>11</sup> such electron transfer could cause significant changes in the PL properties of a toluene/inorganic nanocrystal system via a resonant process. In this article, we present our observation on PL enhancement from *p*-type Si nanocrystals in a toluene suspension. By analyzing the resonant electron transfer between the surface bonding structure and Si nanocrystals, the enhanced PL mechanism can be determined. The calculated results of the electronic states of Si nanocrystals chemisorbed with toluene molecules are corroborated by experiments.

## II. EXPERIMENTS AND SAMPLES

A *p*-type, B-doped Si (100) (1–10 Ω cm) wafer was immersed in a HF solution to remove the surface oxide and then etched in a mixture of 98% CH<sub>3</sub>OH:30% H<sub>2</sub>O<sub>2</sub>:40% HF with a volume ratio of 2:2:1 at a current density of 80 mA/cm<sup>2</sup> for 60 min under room light.<sup>12</sup> Because of the high reactivity between HF and Si oxide, H<sub>2</sub>O<sub>2</sub> catalyzes etching producing smaller Si nanoparticles. The combined effects of the two chemicals leave no oxygen resulting in hydrogen passivation on the Si crystallite surfaces<sup>12</sup> and elimination of defects such as dihydrides and trihydrides as well as impurities.<sup>13</sup> After drying under flowing N<sub>2</sub>, the etched Si wafer was immersed in an ultrasonic toluene bath, in which the porous top layer crumbled into ultrasmall particles to form a suspension of Si nanoparticles.<sup>14</sup> For comparison, the suspension of Si nanoparticles obtained from an *n*-type Si (100) (1–10 Ω cm) wafer was prepared employing the same procedures.

In order to determine the Si crystallite size, we examine the Raman spectra obtained from different locations on the as-etched porous Si sample. The asymmetric Raman peaks appear in the range of 484–511 cm<sup>-1</sup> indicating that the Si crystallites range in size between 1 and 6 nm. It is also noticed that the strongest Raman peak occurs at 493 nm. This implies that most probable Si crystallite size is between 1.5 and 2.0 nm.<sup>15</sup> One of the insets in Fig. 1 shows the transmission electron microscopy (TEM) image of the particle distribution. The same size distribution can be inferred from the TEM image. It can also be observed that some nanocrystals are larger than 5 nm. The other inset in Fig. 1 displays the high-resolution TEM image of a 6 nm particle which exhibits lattice fringes corresponding to the {220} plane of Si, indicating that the Si particle still possesses a diamond structure.

<sup>a)</sup>Author to whom correspondence should be addressed. Electronic mail: [hkxlwu@nju.edu.cn](mailto:hkxlwu@nju.edu.cn)

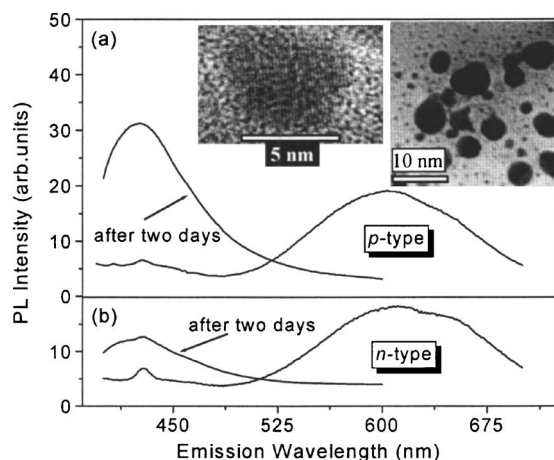


FIG. 1. PL spectra of the toluene suspensions of (a) *p*- and (b) *n*-type Si nanoparticles after storing for <5 min and two days excited by the 380 nm line of a Xe lamp. The insets show the TEM image of the particle distribution and the HRTEM image of a nanoparticle.

### III. EXPERIMENTAL RESULTS AND DISCUSSIONS

Figures 1(a) and 1(b) show the PL spectra of the Si nanoparticles obtained from *p*- and *n*-type wafers suspended in toluene, respectively. The as-made suspensions show only a broad PL band at  $\sim 600$  nm. After they are stored for two days, the  $\sim 600$  nm PL band vanishes and a relatively narrow PL band appears at  $\sim 425$  nm when excited by the 380 nm line of a Xe lamp. The intensity is three times larger in the *p*-type Si nanoparticle suspension than the *n*-type counterpart. If a *p*-type Si wafer with a resistivity of  $0.02 \Omega \text{ cm}$  is used to fabricate porous Si, the PL intensity of the corresponding suspension increases by about six times under the same experimental conditions. This indicates that the PL intensity depends on the hole density in the Si precursor wafer. The  $\sim 600$  nm PL band originates from defect/surface-related states because it has no dependence on the Si crystallite sizes and excitation wavelength, and its PL excitation (PLE) spectrum remains unchanged with the excitation wavelength.<sup>16–19</sup> Thus, chemisorption of toluene leads to the removal of some defect states on the Si nanocrystal surface. In order to study the origin of the  $\sim 425$  nm PL, we examine a series of PL spectra by selecting different excitation wavelengths and the results are displayed in Fig. 2 (all the spectra have been corrected for the sensitivity of the measurement system). These PL spectra show three main features. (1) The blue PL peak wavelength increases with the excitation wavelength, thereby ruling out the oxide mechanism. It should be mentioned that several PL spectra have a sharp top that can be calculated to be the Raman scattering signals of toluene. They overlap with a broad PL band. (2) The 425 nm PL intensity has a maximum. If we adopt the quantum confinement theory for Si nanocrystals with sizes of 1.5–2.0 nm,<sup>16,18</sup> the 425 nm PL peak can be inferred to derive from the band-to-band recombination in the quantum confined Si nanocrystals. Since most Si nanocrystals in the suspension have sizes of 1.5–2.0 nm, it is understandable that the 425 nm PL band has a maximum intensity. (3) The linewidth of the PL spectrum decreases with increasing excitation wavelength. If different excitation energies can gen-

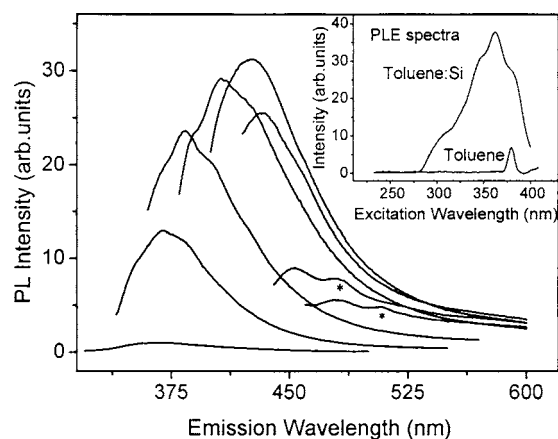


FIG. 2. PL spectra of the toluene suspension of *p*-type Si nanoparticles after storing for two days excitation by the 300, 320, 340, 360, 380, 400, 420, or 440 nm lines of a Xe lamp. The peaks marked by (\*) are the Raman signals. The inset shows the PLE spectra of the suspension and pure toluene solution excited by the 425 nm.

erate carriers with different energies which depend on the particle size, the decrease in the linewidth should mainly be due to the shrunk size distribution of the excited nanocrystals. This point is more evident in the two PL spectra excited by the 420 and 440 nm lines. They have low intensities and narrow linewidths due to the small number of particles with large sizes (the Raman peaks have been separated from the PL bands).

The above results clearly demonstrate that the tunable violet-blue PL arises from the band-to-band recombination in the quantum confined Si nanocrystals. To study the photoexcited process of carriers, the PLE spectra of the suspension and pure toluene are acquired and the different emission wavelengths are analyzed. The typical result is presented in the inset of Fig. 2. The photoexcited carriers are not present in toluene because the absorption edge of toluene is  $\sim 280$  nm.<sup>20</sup> However, the PLE spectrum of the toluene suspension shows a broadband which overlaps with some small peaks at 310, 345, and 356 nm as well as an enhanced Raman peak at 376 nm (an aromatic CH stretching vibration mode). The broad PLE band can be attributed to the band-to-band absorption and is frequently observed in porous Si.<sup>16,19</sup> The three small peaks at 310, 345, and 356 nm can be confirmed to be the optical absorption bands, not the Raman modes. Their emergence indicates that some of the toluene molecules are in a specific electronic structure or state that may be associated with the surface bonding structure of the Si nanocrystal. Hence, the photoexcited carriers not only are present in the quantum confined Si crystallite cores but also occur at the Si crystallite surface. This result can help to explain the intensity enhancement of the PL spectra obtained from the suspension of *p*-type Si nanoparticles. Figure 3 shows the structural models and energy band diagrams of both Si nanoparticles and the three stable dissociated configurations of Si nanoparticles chemisorbed with toluene.<sup>10</sup> After the electrons in the surface states are excited by light, they transfer to the conduction band of the Si nanocrystal with a widened band gap via direct electron exchange mechanism (Dexter transfer).<sup>21</sup> These electrons, together

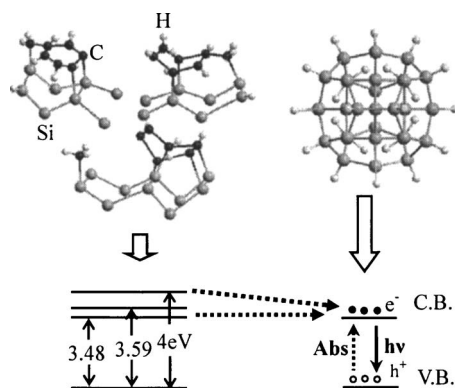


FIG. 3. Structural models of the Si nanocrystals and three stable dissociated configurations for Si nanocrystals chemisorbed with toluene (Ref. 10). The energy level schematic diagrams show the excitation, transfer, and recombination processes of electrons.

with other electrons in the conduction band of the Si nanocrystals which are simultaneously produced by band-to-band absorption, recombine radiatively with the holes in the valence band of the Si nanocrystals to produce the observed blue emission. In our current experiments, the Si nanocrystals and their surface structure act as acceptors and donors, respectively. Overlap of the acceptor and donor electron energy levels, their small space separation, and the long lifetime of electronic excitation of the donor play an important role in the efficient electron transfer.<sup>21,22</sup> Since the band gap of the Si nanoparticle depends on its size, the measured PL spectrum shows an evident dependence on the Si particle size. Based on the above description, the reason why the *p*-type Si nanoparticles suspended in toluene has larger PL intensity is that the *p*-type Si nanoparticles have a larger hole density.

#### IV. THEORETICAL CALCULATION

The analysis described in the previous paragraphs is qualitative, because the resonant electron transfer from the surface structure to the Si nanoparticles and radiative recombination of electrons and holes in the Si nanoparticles need to meet the corresponding selection rules. To provide theoretical evidence of the electronic states, we calculate the density of the electronic states of the suspension system. The study of chemisorption of toluene on the Si (100) surface has indicated that the C–H bond of the methyl (CH<sub>3</sub>) group is cleaved and the hydrogen is bonded to the Si surface. This is described as a proton abstraction reaction.<sup>10</sup> The excess negative charge in the C atom can transfer to the Si atom along a new C–Si bond. If the Si nanoparticle is in toluene, the surface of the Si particle can be passivated by H atoms and some Si atoms can bond with the methyl group. It may be argued that the original electrochemical etching process should completely passivate the particle surfaces with H atoms. Therefore, further H or CH<sub>3</sub> passivation in the toluene solution is difficult to take place. However, this is not the case. It is known that a porous Si layer formed during electrochemical etching consists of many H-surface passivated Si dendrites. These dendrites which have diameters of micrometers further comprise Si nanocrystals with sizes of

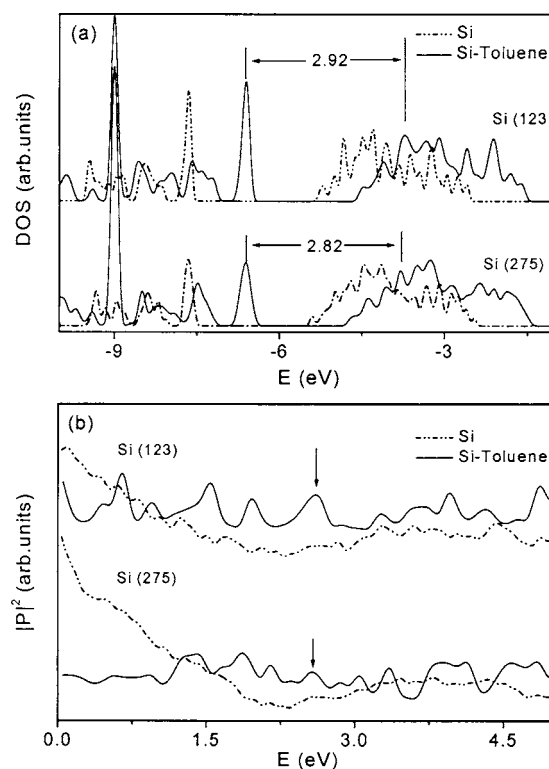


FIG. 4. (a) Densities of states for different Si nanospheres. The dotted lines are for pure Si spheres composed of 123 and 275 Si atoms. The solid lines are for two passivated Si spheres. One consists of 123 Si atoms, 72 hydrogen atoms, and 16 methyl (CH<sub>3</sub>) molecules, and the other consists of 275 Si atoms, 120 hydrogen atoms, and 52 methyl molecules. (b) The absolute squared optical matrix element as a function of the transmission energy for the different cases in (a).

1–8 nm.<sup>23,24</sup> The surface of these Si nanocrystals are typically unpassivated with H atoms. When they crumble and disperse in a toluene solution, a large number of fresh Si sites form and can react with hydrogen and the methyl group. Using the method of linear combination of atomic orbitals (LCAO), we can obtain the density of states [Fig. 4(a)] and the absolute squared optical matrix element [Fig. 4(b)] for the Si nanospheres with and without H and methyl passivation. The calculation was conducted using the LCAO method and tight-binding parameters. The levels of *3s* and *3p* states in a Si atom are  $\epsilon_s^{\text{Si}} = -13.5$  eV and  $\epsilon_p^{\text{Si}} = -7.58$  eV and the nearest neighbor hopping integrals are  $V_{ss\sigma}^{\text{Si}} = -2.08$  eV,  $V_{sp\sigma}^{\text{Si}} = 2.48$  eV,  $V_{pp\sigma}^{\text{Si}} = 2.72$  eV, and  $V_{pp\pi}^{\text{Si}} = -0.72$  eV.<sup>25</sup> The levels of *2s* and *2p* states in a C atom are  $\epsilon_s^{\text{C}} = -17.52$  eV and  $\epsilon_p^{\text{C}} = -8.97$  eV and the nearest neighbor hopping integrals are  $V_{ss\sigma}^{\text{C}} = -2.83$  eV,  $V_{sp\sigma}^{\text{C}} = 3.73$  eV,  $V_{pp\sigma}^{\text{C}} = 6.59$  eV, and  $V_{pp\pi}^{\text{C}} = -1.64$  eV.<sup>26</sup> The level of hydrogen  $\epsilon_s^{\text{H}} = -13.6$  eV.<sup>27</sup> The nearest neighbor hopping integrals between Si and H are  $V_{ss\sigma}^{\text{Si-H}} = -4.075$  eV and  $V_{sp\sigma}^{\text{Si-H}} = 4.0$  eV;<sup>27</sup> the nearest neighbor hopping integrals between C and H are  $V_{ss\sigma}^{\text{C-H}} = -7.8$  eV and  $V_{sp\sigma}^{\text{C-H}} = 10.24$  eV.<sup>26</sup> In our calculation, two Si nanospheres containing 123 (1.6 nm) and 275 Si atoms (2.1 nm) are considered and each atom on the surface has one or two dangling bonds. For the passivated Si nanospheres, the surface atoms with two dangling bonds are passivated by H and those with one dangling bond react with the methyl group.

The empirical tight-binding parameters of Si are from Ref. 25, Si-H data are from Ref. 27, and the C-H and Si-C data are calculated according to Ref. 26.

The energy gaps of the Si spheres before or after passivation are always smaller for larger particles, as shown in Fig. 4(a), and it suggests the quantum confinement effect. Both the valence band top and conduction band move to a higher energy (right side) after passivation. For the passivated Si spheres with sizes of 1.6 and 2.1 nm, the energies between the top of the valence band and the obvious peak in conduction band are 2.92 and 2.82 eV, respectively, and they are consistent with our experimental results. In Fig. 4(b), no obvious peak can be found from the Si nanosphere without passivation, but some peaks appear after passivation. Among these peaks, only the peak indicated by an arrow corresponds to the observed emission. Our calculation further proves that when Si nanoparticles are chemisorbed with toluene molecules, the quantum confinement effect occurs in such small Si spheres and the intensity of the corresponding PL spectra increases.

## V. CONCLUSION

We have observed efficient resonant electron transfer from the surface bonding structure to the conduction band of the quantum confined Si nanocrystals suspended in toluene. Based on the electron transfer mechanism, the enhancement of the photoluminescence intensity originates from the band-to-band recombination in the *p*-type Si nanocrystal suspension in toluene. The electron energy levels in the Si nanocrystals chemisorbed with toluene molecules are calculated using the LCAO method and the obtained density of states are in good agreement with the experimental PL results.

## ACKNOWLEDGMENTS

This work was supported by the grants (Grant Nos. 10225416, 60576051, and 80476038) from the National Natural Science Foundation of China and the LAPEM. Partial support was also from the Major State Basic Research Project No. G001CB3095 of China and City University of Hong Kong Direct Allocation Grant No. 9360110.

- <sup>1</sup>N. C. Greenham, X. G. Peng, and A. P. Alivisatos, *Phys. Rev. B* **54**, 17628 (1996).
- <sup>2</sup>D. S. Ginger and N. C. Greenham, *Phys. Rev. B* **59**, 10622 (1999).
- <sup>3</sup>J. M. Rehm, G. L. McLendon, Y. Nagasawa, K. Yoshihara, J. Moser, and M. Gratzel, *J. Phys. Chem.* **100**, 9577 (1996).
- <sup>4</sup>M. C. Schlamp, X. G. Peng, and A. P. Alivisatos, *J. Appl. Phys.* **82**, 5837 (1997).
- <sup>5</sup>C. R. Kagan, D. B. Mitzi, and C. D. Dimitrakopoulos, *Science* **286**, 945 (1999).
- <sup>6</sup>S. Coe, W. K. Woo, M. Bawendi, and V. Bulovic, *Nature (London)* **420**, 800 (2002).
- <sup>7</sup>W. U. Huynh, J. J. Dittmer, and A. P. Alivisatos, *Science* **295**, 2425 (2002).
- <sup>8</sup>J. M. Rehm, G. L. McLendon, and P. M. Fauchet, *J. Am. Chem. Soc.* **118**, 4490 (1996).
- <sup>9</sup>D. L. Fisher, J. Harper, and M. J. Sailor, *J. Am. Chem. Soc.* **117**, 7846 (1995); J. H. Song and M. J. Sailor, *ibid.* **119**, 7381 (1997).
- <sup>10</sup>F. Costanzo, C. Sbraccia, P. L. Silvestrelli, and F. Ancilotto, *J. Phys. Chem. B* **107**, 10209 (2003) and references therein.
- <sup>11</sup>For a review, see A. G. Cullis, L. T. Canham, and P. D. J. Calcott, *J. Appl. Phys.* **82**, 909 (1997) and references therein.
- <sup>12</sup>Z. Yamani, H. Thompson, L. A. Hassan, and M. H. Nayfeh, *Appl. Phys. Lett.* **70**, 3404 (1997).
- <sup>13</sup>G. Belomoin, E. Rogozhina, J. Therrien, P. V. Braun, L. Abuhassan, M. H. Nayfeh, L. Wagner, and L. Mitas, *Phys. Rev. B* **65**, 193406 (2002).
- <sup>14</sup>M. Jarrold and E. Honea, *J. Phys. Chem.* **95**, 9181 (1991).
- <sup>15</sup>X. L. Wu, Y. F. Mei, G. G. Siu, K. L. Wong, K. Moulding, M. J. Stokes, C. L. Fu, and X. M. Bao, *Phys. Rev. Lett.* **86**, 3000 (2001).
- <sup>16</sup>X. L. Wu, S. J. Xiong, D. L. Fan, Y. Gu, X. M. Bao, G. G. Siu, and M. J. Stokes, *Phys. Rev. B* **62**, R7759 (2000).
- <sup>17</sup>S. S. Deng, X. L. Wu, Z. Y. Zhang, Y. F. Mei, Y. Yang, H. Chen, and X. M. Bao, *Phys. Lett. A* **299**, 299 (2002).
- <sup>18</sup>M. V. Wolkin, J. Jorne, P. M. Fauchet, G. Allan, and C. Delerue, *Phys. Rev. Lett.* **82**, 197 (1999).
- <sup>19</sup>Y. H. Xie, W. L. Wilson, F. M. Ross, J. A. Mucha, E. A. Fitzgerald, J. M. Macaulay, and T. D. Harris, *J. Appl. Phys.* **71**, 2403 (1992).
- <sup>20</sup>H. Du, R. C. A. Fuh, J. Z. Li, L. A. Corkan, and J. S. Lindsey, *Photochem. Photobiol.* **68**, 141 (1998).
- <sup>21</sup>G. Kodis, P. A. Liddell, L. de la Garza, P. C. Clausen, J. S. Lindsey, A. L. Moore, T. A. Moore, and D. Gust, *J. Phys. Chem. A* **106**, 2036 (2002).
- <sup>22</sup>X. L. Wu, M. X. Liao, S. S. Deng, and G. G. Siu, *J. Chem. Phys.* **121**, 991 (2004).
- <sup>23</sup>M. W. Cole, J. F. Harvey, R. A. Lux, D. W. Eckart, and R. Tsu, *Appl. Phys. Lett.* **60**, 2800 (1992).
- <sup>24</sup>X. M. Bao, *Prog. Phys. (in Chinese)* **13**, 280 (1993).
- <sup>25</sup>P. Vogl, H. P. Hjalmarson, and D. J. Dow, *J. Phys. Chem. Solids* **44**, 365 (1983).
- <sup>26</sup>W. A. Harrison, *Electronic Structure and the Properties of Solids* (Freeman, San Francisco, 1980).
- <sup>27</sup>H. X. Fu, L. Y. Ling, and X. D. Xie, *Phys. Rev. B* **48**, 10978 (1993).